Cellular and Molecular Life Sciences (2026) 83:199
https://doi.org/10.1007/s00018-026-06089-1

ORIGINAL ARTICLE

Aiolos and Eos drive distinct human TH17 functional states

Silvia Cerboni[1] · Leila Mohammadnezhad[2] · Komal Agrawal[1] · Ramachandramouli Budida[1] · Ilenia Papa[3] · Silvia Gaggero[2] · Joel Dulong[3] · Anna Cole[4] · Anja Mezger[5] · Bingyu Yan[6] · Zonghao Zhang[7] · Elisabeth Israelsson[1] · Petr Volkov[8] · Songyuan Li[5] · Eva F. Caceres[8] · Malo Leprohon[2] · Mojtaba Shekarkar Azgomi[2] · Yue Cui[1] · Svitlana Salemio[1] · Mike Firth[9] · Leif Wigge[8] · Anna Rudin[10] · Hanna Grindebacke[11] · Marcello Maresca[5] · Chrystal Paulos[4] · Franck Morschhauser[12] · Salomon Manier[2,12] · Majid Kazemian[6,12] · Arian Laurence[13] · Michael Hühn[14] · Ulf Gehrmann[1] · Karin Tarte[3] · Suman Mitra[2]

Received: 28 August 2025 / Revised: 5 January 2026 / Accepted: 9 January 2026

Abstract

CD4+ T helper (TH)-17 cells play a pivotal role in mucosal immune defense and are implicated in autoimmune diseases and cancer. Although Th17 cell plasticity is well-studied in mice, the factors driving their transition between pro-inflammatory and immunomodulatory states in humans remain less understood. Our study explored the transcriptional and epigenetic landscapes of single-cell cultures of human memory TH17 cells, focusing on clones that produce either immunomodulatory IL-10 or pro-inflammatory IFNγ and IL-22. We found that IL-10+ TH17 cells exhibit a T cell exhaustion-like profile with increased CTLA-4 expression and reduced IL-2 levels, while Ikaros zinc finger (IkZF) transcription factors, Aiolos and Eos, are differentially expressed in IL-10+ and IL-22+ TH17 cells, respectively. While exogenous IL-2 promotes IL-10 production in TH17 cells, lenalidomide induces IL-2 and promotes inflammatory TH17 cells, shifting TH17 cells towards a pro-inflammatory phenotype by reducing IL-10 and increasing IL-22 and IFNγ levels. Conversely, upregulation of Eos enhanced pro-inflammatory cytokine production. These findings highlight the crucial role of IkZF transcription factors in regulating human TH17 cell functions. Moreover, single-cell RNA sequencing of PBMCs from lenalidomide-treated patients confirmed an enrichment of inflammatory signatures, including interferon and IL-2/STAT5 pathways in TH17 cells. The ability to modulate this axis through targeted interventions, such as lenalidomide-induced Aiolos degradation or enforced Eos expression, presents new therapeutic opportunities for managing TH17 cell states in cancer and autoimmune diseases.

Keywords TH17 cells · IkZF transcription factors · Lenalidomide · IL-10 · IL-22 · T cell plasticity

TH17 cells characterized by the ability to express interleukin (IL)−17 when activated, play a critical role in mucosal immunity [1, 2]. Conversely, TH17 cells are also implicated in the pathophysiology of autoimmunity and inflammatory disorders [3, 4] and cancer [5–8], attracting interest in elucidating the biochemical mechanisms that regulate TH17 behavior.

In humans, TH17 cell development differs substantially from murine systems. While mouse Th17 cells differentiate optimally in the presence of TGF-β and IL-6, human TH17 cell differentiation protocols typically require IL-1β and IL-23 stimulation, with TGF-β paradoxically inhibiting rather than promoting human TH17 cytokine expression. These cytokine requirements highlight fundamental species differences in TH17 biology. Similarly, while IL-2 consistently inhibits Th17 differentiation in mice [9], its role in human TH17 cell function remains controversial, with both positive and negative effects on IL-17 expression reported depending on experimental conditions [10, 11].

Human TH17 cells exhibit remarkable functional heterogeneity that may differ from mouse Th17 cells. Classical human TH17 cells are characterized by expression of IL-17 and immuno-modulatory genes normally associated with Tregs (e.g. IL-10, CTLA-4, LRRC32) and the transcription

Silvia Cerboni, Leila Mohammadnezhad, Komal Agrawal and Ramachandramouli Budida contributed equally to this work.

Arian Laurence and Suman Mitra are senior authors.

Extended author information available on the last page of the article

Published online: 01 April 2026

factors (TFs) *MAF* and *IKZF3* (encoding for Aiolos), which have been implicated in *IL10* gene regulation in human TH cells [12–14]. IL-10-producing TH17 cells may contribute to tissue homeostasis as loss-of-function mutations in the IL-10 or IL-10R genes lead to pediatric onset of IBD in humans [15]. By contrast, non-classical TH1/17 cells that express both IL-17 and IFNγ have been found at sites of inflammation [16]. Given their transcriptional similarity to murine pathogenic Th17 cells [17], human TH1/17 cells are believed to be pro-inflammatory and contribute to the pathogenesis of human autoimmune diseases such as psoriasis, psoriatic arthritis, and other spondyloarthritides [13].

Pro-inflammatory TH17 cells show features of both TH1 and TH17 cells as they co-express the TFs ROR-γt and T-bet as well as IL-12Rβ2 and IL-23R [18–21]. They are characterized by co-expression of pro-inflammatory cytokines such as granulocyte-macrophage colony-stimulating factor (GM-CSF), IL-26, CCL20 and IL-22 [22]. Moreover, TH17-derived IL-22 plays a dual role, contributing to both tissue repair and the exacerbation of inflammatory diseases like psoriasis [23].

Despite this growing understanding of human TH17 functional heterogeneity, the transcriptional mechanisms governing the balance between regulatory and inflammatory TH17 states remain poorly defined. The IKAROS zinc finger (IkZF) transcription factor family, which includes IKZF1 (Ikaros), IKZF3 (Aiolos), and IKZF4 (Eos) are associated with chromatin remodeling [24]. This family has emerged as a key regulator of pro- and non-inflammatory TH17 cells [25]. In mice, Aiolos has been shown to promote Th17 differentiation by directly silencing *Il2* expression and enhancing IL-17 expression [26]. Additionally, CD4+ T cells require Ikaros to inhibit their differentiation toward a pathogenic cell fate [27] and to regulate IL-10 expression [28]. In contrast to Ikaros and Aiolos, Eos has been implicated in negatively regulating Th17 differentiation and function as inhibition of Eos expression by the miRNA miR-17 was shown to enhance Th17 cell development [28]. However, the specific roles of these transcription factors in human TH17 cell heterogeneity and function remain largely unexplored.

In our study, we dissected the heterogeneity within human TH17 cell populations by sorting and clonally expanding TH17 cells based on their production of IL-17 in conjunction with either IL-10 or IL-22. We found that IKZF1 (Ikaros) and IKZF3 (Aiolos) were predominantly expressed in TH17-IL-10+ cells, while IKZF4 (Eos) was specifically expressed in TH17-IL-22+/IFNγ+ cells. Our research revealed that pharmacological degradation of Ikaros and Aiolos or forced expression of Eos induced an inflammatory TH17 phenotype, expressing IL-17, IFNγ, and IL-22. Stimulation with exogenous IL-2 significantly increased IL-10 production in TH17 cells. These data provide novel insights into the unique regulatory mechanisms of human TH17 cells, which are distinct from those identified in established murine models. The findings underscore the potential for targeted therapeutic interventions in autoimmune and inflammatory disorders.

Results

Differential regulation of IL-22 and IL-10 expression in human TH17 subclones

In this study, we aimed to establish and characterize distinct clonal populations of human memory TH17 cells expressing either IL-22 or IL-10 to better understand the regulatory mechanisms and biological functions of these cytokines in different TH17 functional states. To achieve this, we selected TH17 clones based on their specific expression of IL-22 or IL-10 in both resting (day 0) and recently activated (day 5, 5 days after re-stimulation) states (Fig. 1A and Fig. S1). All selected clones highly expressed IL-17 at day 0 but marginally reduced IL-17 expression at day 5 following activation by anti-CD3/CD28 microbeads (Fig. 1B, C). TH17-IL-10+ clones maintained high levels of IL-10 expression at both resting and activated state with only a fraction of cells expressing IFNγ or IL-22 (Fig. 1B, C). On the contrary, clones that expressed IL-22 also expressed IFNγ but did not express IL-10, defining a distinct human subset from the previously described TH17-IL-10+ subset [14] and demonstrating reciprocal regulation of IL-10 and IL-22 by TH17 subclones.

These results suggested that the expression of IL-22 and IL-10 in TH17 cells is differentially regulated and may be associated with distinct biological roles. The TH17-IL-10+ subset appeared to maintain a more stable phenotype, with consistent IL-10 expression and minimal co-expression of other cytokines, whereas the TH17-IL-22+/IFNγ+ subset exhibited co-expression of IFNγ and a lack of IL-10 expression.

Distinct epigenetic and transcriptomic profiles of the TH17-IL-22+/IFNγ+ and TH17-IL-10+ memory subsets

To explore the molecular mechanisms regulating functional heterogeneity of TH17-IL22+/IFNγ+ versus -IL-10+ subsets, we generated ATAC-seq and RNA-seq data sets from both TH17 clone subsets before and after re-stimulation. Principal component analysis (PCA) of both the chromatin landscape and RNA expression profiles demonstrated a clear separation between TH17-IL-22+/IFNγ+ and TH17-IL-10+ clones, both at day 0 and day 5 (Fig. 2A, B).

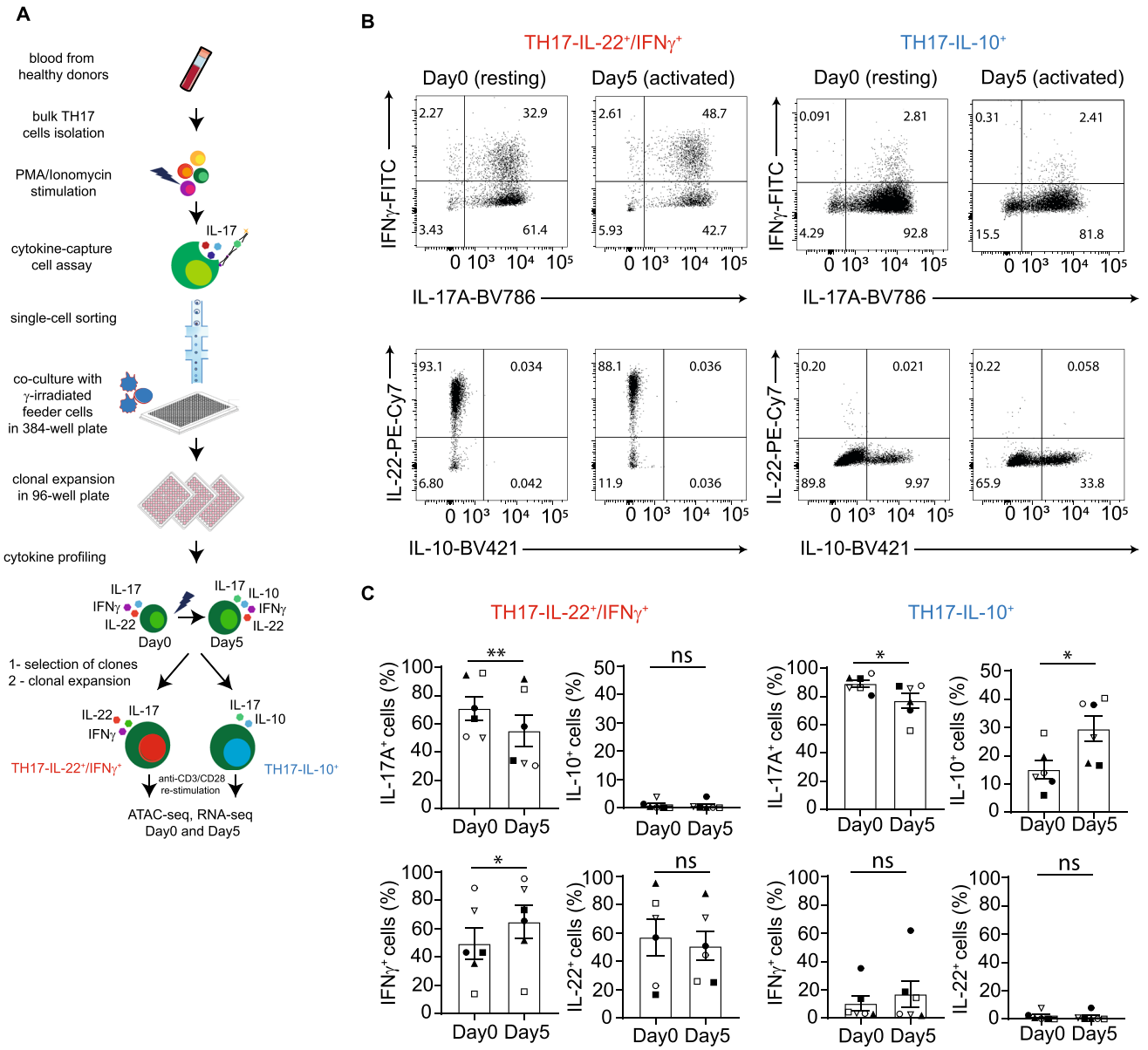

Fig. 1 Identification of Distinct Human TH17 Cell Subsets and Generation of Stable TH17 Clones from PBMC for Functional Characterization. **A** Schematic representation of the workflow to generate T_H17-IL22$^+$/IFNg$^+$ and T_H17-IL-10$^+$ clones used to perform bulk ATAC-seq and RNA-seq data sets. In brief, peripheral blood mononuclear cells (PBMCs) were isolated from fresh blood using density gradient centrifugation. The samples were enriched for CD4+CCR6+CXCR3-TH17 cells, referred to as "bulk TH17 cells." Viable IL-17-producing cells were isolated by flow cytometry following a 3-hour stimulation with PMA and ionomycin using a IL-17 capture assay. The single TH17 cell clones were sorted into 384-well plates and expanded with allogeneic γ-irradiated feeder cells and phytohemagglutinin in complete medium containing IL-2. After approximately ten days, clones were transferred to 96-well plates for expansion, and following 2–3 weeks, their cytokine profiles were analyzed. T cell clones were then evaluated at two stages: day 0 (resting state) and day 5 (activated state). On day 5, they were stimulated for 48 hours with anti-CD3 and CD28, followed by an additional 3 days in uncoated plates. On both evaluation days, cells underwent further stimulation — 5 hours for protein analysis and 2 hours for RNA and chromatin-accessibility (ATAC-seq) analysis. Only TH17 clones exhibiting a stable cytokine profile after two rounds of resting and reactivation were selected for RNA-seq and ATAC-seq analysis. **B** Intracellular staining of IL-17 and IFNγ (top) and IL-22 and IL-10 (bottom) in a T_H17-IL10$^+$ clone (right) and a T_H17-IL22$^+$/IFNg$^+$ clone (left) in the resting state (Day 0) and 5 days post-activation (Day 5). Numbers in quadrants indicate percent cells. **C** Frequency of IL-17+, IL-10+, IFNγ+, and IL-22+ cells among 6 independent TH17-IL-22$^+$/IFNγ$^+$ (left) and TH17-IL-10$^+$ (right) clones at Day 0 and Day 5. Each symbol represents an individual T cell clone ($n=6$); data are shown as mean ± s.e.m. *$P<0.05$, **$P<0.01$ (one-way ANOVA). TH17 clones were selected for RNA and ATAC-seq analysis based on the following criteria: ≥50% IL-17A+ cells at Day 0, ≥15% IL-22+ cells at Day 0 and Day 5, ≥15% IFNγ+ cells at Day 0 and Day 5 for TH17-IL-22$^+$/IFNγ$^+$ clones; ≥50% IL-17A+ cells at Day 0, ≥15% IL-10+ cells at Day 5 for TH17-IL-10$^+$ clones

Differential peak enrichment analysis of the ATAC-seq data revealed distinct chromatin accessibility patterns between the two subsets at both time points (Fig. 2C). We identified *SREBF2*, *ZNF382* and *IKZF1* binding motifs as enriched in TH17-IL-22+/IFNγ+ cells at day 0 (Fig. 2D and Supplementary Table.1) using the chromVAR tool. SREBF2 is a transcription factor (TF) which regulates lipid metabolism and favors TH17 differentiation [29], and ZNF382 encodes a zinc finger containing TF which has been reported to down-regulate STAT3 [30]. IKZF1, but not SREBF2 and ZNF382, binding sites were also enriched in TH17-IL-22+/IFNγ+ as compared to TH17-IL-10+ clones at day 5 (Fig. 2E and Supplementary Table.2) prompting us to analyze the genes associated with IKZF1 motifs. In total, 1515 genes were identified in regions with prominent ATAC-seq peaks in TH17-IL-22+/IFNγ+ clones at day 0, of which 689 genes contain an IKZF1 binding site (Supplementary Table 3). The list contained many cytokines and receptors (e.g. IL-2, IL-21, IL-22, IFNγ, IL-23R) associated with pro-inflammatory TH17 cells, suggesting that IKZF1 might have a role in the transcriptional regulation of this TH17 cell subset. Pathway enrichment analysis using Enrichr [31](KEGG database) revealed that IKZF1-motif-containing genes were strongly enriched in T cell and inflammatory pathways, with Th17 cell differentiation as the most significant ($p = 7.77 \times 10^{-7}$). Additional enriched pathways included inflammatory bowel disease, T cell receptor signaling, NF-κB signaling, and Th1/Th2 differentiation (all $p < 0.01$), confirming a role for IKZF1-binding genes in T cell activation and inflammation (Fig. S2A,B).

Next, we performed differential gene expression analysis between the two TH17 subsets at both time points (Fig. 2F). This analysis revealed distinct transcriptional programs in each subset, with the number of differentially expressed genes approximately doubling upon activation, indicating enhanced transcriptional divergence after stimulation. TH17-IL-10+ cells showed a greater number of upregulated genes compared to TH17-IL-22+/IFNγ+ cells at both timepoints. Most importantly, very few genes were shared between both subsets across timepoints, demonstrating that these represent fundamentally distinct functional programs rather than variations of a common transcriptional state (Supplementary Tables 4 & 5).

Gene Set Enrichment Analysis (GSEA) using a known TH17-IL-10$^-$ and TH17-IL-10$^+$ transcriptional signature dataset validated the clonal signature of our TH17-IL-22$^+$/IFNγ$^+$ versus TH17-IL-10$^+$ subsets. TH17-IL-10$^+$ clones closely resembled the previously established TH17-IL-10$^+$ clones [14], whereas TH17-IL-22$^+$/IFNγ$^+$ clones showed only a partial overlap with the TH17-IL-10$^-$ signatures (Fig. S3A). Notably, by day 5 post-activation, the distinction between IL-22 and IL-10 profiles became less clear, suggesting a potential influence of activation on their gene expression (Fig. S3B).

Fig. 2 Distinct Chromatin Landscape and Expression Profile of TH17-IL-22$^+$/IFNγ$^+$ and TH17-IL-10$^+$ Clones. **A**, **B** PCA plot of bulk ATAC-seq (**A**) and RNAseq data (**B**) comparing TH17-IL-22$^+$/IFNγ$^+$ and TH17-IL-10+ clones at Day 0 and Day 5 following 2 hours of anti-CD3 and anti-CD28 restimulation. **C** Heatmaps displaying differential peak enrichment in memory TH17-IL-22$^+$/IFNγ$^+$ (orange/red) vs TH17-IL-10$^+$ (light/dark blue) cells at Day 0 and Day 5, respectively. **D**, **E** Top transcription factor (TF) motifs enriched in TH17-IL-22$^+$/IFNγ$^+$ or TH17-IL-10$^+$ clones at Day 0 and Day 5 using chromVar analysis, revealing an enrichment of IKZF binding in TH17-IL-22$^+$/IFNγ$^+$ cells compared to TH17-IL-10$^+$ cells. **F** Venn diagram of differentially expressed genes between the two TH17 subsets at Day 0 and Day 5. **G**, **H** Bulk RNA-seq analysis of TH17-IL-22$^+$/IFNγ$^+$ and TH17-IL-10$^+$ cells at Day 0 and Day 5 after 2 hours of restimulation with anti-CD3 and anti-CD28, presented as scatter plots (left) and bar plots (right) of the expression in TH17-IL-22$^+$/IFNγ$^+$ relative to TH17-IL-10$^+$ cells (log2 fold change) plotted against the difference in mean expression values. Symbol colors indicate genes differentially expressed with padj <0.05 and 0.5-fold or more in TH17-IL22$^+$/IFNγ$^+$ cells (red, up in IL-22$^+$/IFNγ$^+$) or TH17-IL-10$^+$ (blue, up in IL-10+). **I** IKZF transcription factors gene expression normalized to GAPDH in TH17-IL-22$^+$/IFNγ$^+$ or TH17-IL-10$^+$ clones at Day 0 and Day 5. Each symbol represents an individual TH17 clone. Data are combined from three or more independent experiments. For ATAC-seq: $n = 6$ for TH17-IL-22$^+$/IFNγ$^+$ clones and $n = 3$ for TH17-IL-10$^+$ clones (three TH17-IL-10$^+$ clones were excluded due to insufficient cell numbers). For RNA-seq: $n = 6$ for both TH17-IL-22$^+$/IFNγ$^+$ and TH17-IL-10$^+$ clones; mean ± s.e.m. $^*P < 0.05$, $^{**}P < 0.01$, $^{***}P < 0.001$, and $^{****}P < 0.0001$ (one-way ANOVA). **J** UMAP projection of module scores of IL-22-regulated genes (left) and IL-10-regulated genes (right) derived from the bulk RNA-seq data of TH17-IL22$^+$/IFNγ$^+$ and TH17-IL-10$^+$ clones. (see Supplementary Tables 4 and 5 for gene lists)

To characterize the two subsets, we performed over-representation analysis (ORA) on differentially expressed genes in TH17-IL-22+/IFNγ+ vs TH17-IL-10+ clones (Supplementary Tables 6 & 7). We found that the genes significantly overexpressed in TH17-IL-22+/IFNγ+ cells encode for molecules involved in inflammatory response, leukocyte-mediated cytotoxicity, and STAT phosphorylation pathways at both day 0 and day 5 (Fig. S3C). A deeper investigation of the top 10 enriched pathways revealed that several cytotoxicity-related genes such as PRF1, GZMA, GZMH, INFG and GNLY were overexpressed together with multiple chemokines such as CCL1 and XCL1 in TH17-IL-22+/IFNγ+ cells (Fig. S3D, E). TH17-IL-22+/IFNγ+ clones expressed significantly higher mRNA levels of the cytokine genes *IL22, IL2, CSF2, IFNG, TNF*, confirming their pro-inflammatory profile both at day 0 and day 5 (Fig. 2G, H). To determine whether TH17-IL-22$^+$/IFNγ$^+$ cells exhibit a Th1-like transcriptional profile, we performed GSEA using a Th1 signature [32] on ranked differentially expressed genes. By day 5, TH17-IL-22$^+$/IFNγ$^+$ cells showed stronger Th1 signature enrichment than TH17-IL-10$^+$ cells, indicating a Th1-skewed transcriptional

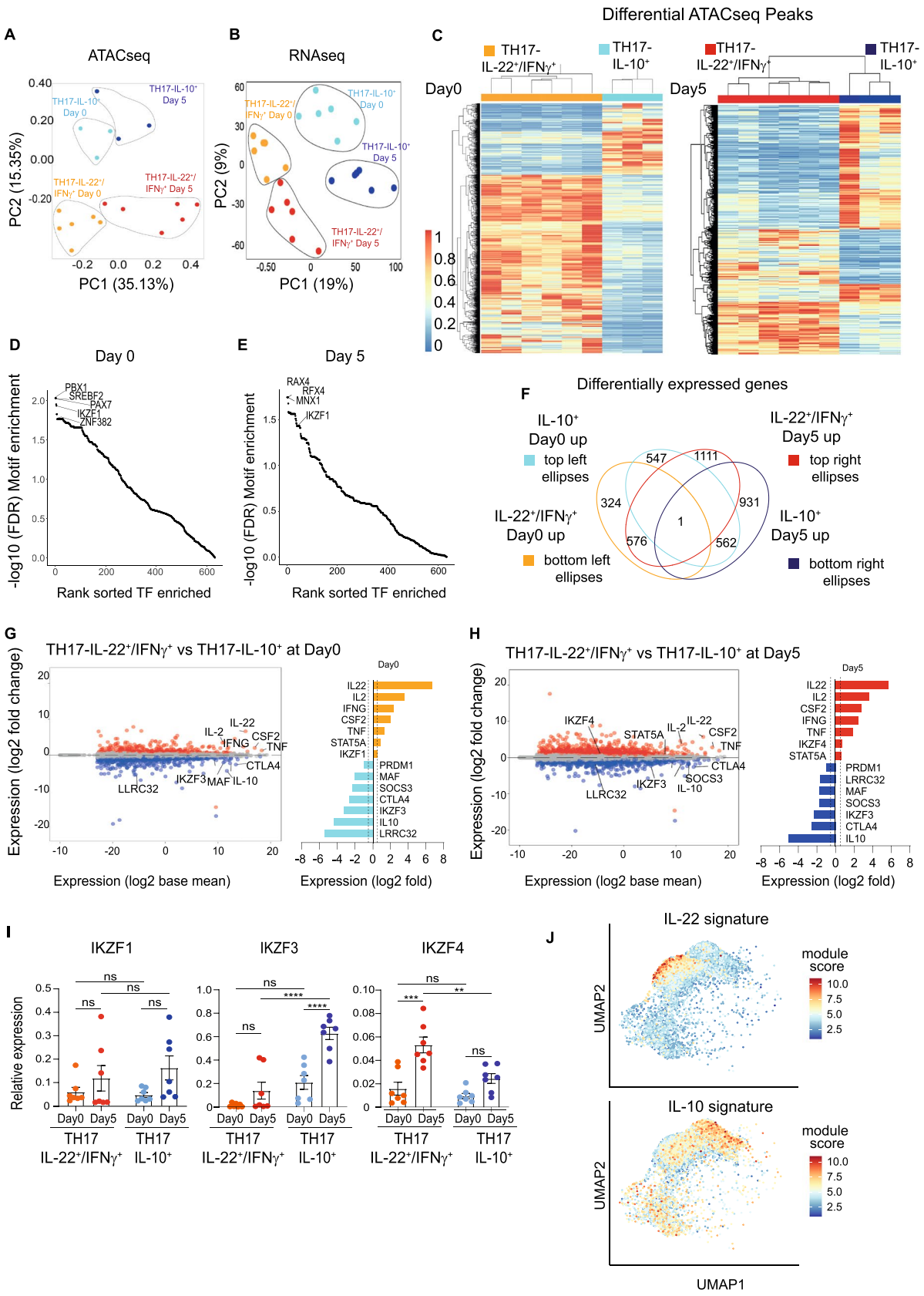
A
ATACseq
PC2 (15.35%)
PC1 (35.13%)
TH17-IL-10+ Day 0
TH17-IL-10+ Day 5
TH17-IL-22+/IFNγ+ Day 0
TH17-IL-22+/IFNγ+ Day 5
B
RNAseq
PC2 (9%)
PC1 (19%)
C
Differential ATACseq Peaks
TH17-IL-22+/IFNγ+
TH17-IL-10+
Day0
Day5
D
Day 0
-log10 (FDR) Motif enrichment
PBX1
SREBF2
PAX7
IKZF1
ZNF382
Rank sorted TF enriched
E
Day 5
RAX4
RFX4
MNX1
IKZF1
F
Differentially expressed genes
IL-10+ Day0 up
top left ellipses
IL-22+/IFNγ+ Day5 up
top right ellipses
IL-22+/IFNγ+ Day0 up
bottom left ellipses
IL-10+ Day5 up
bottom right ellipses
547
1111
324
931
1
576
562
G
TH17-IL-22+/IFNγ+ vs TH17-IL-10+ at Day0
Expression (log2 fold change)
Expression (log2 base mean)
Expression (log2 fold)
IL-22
IL-2
IFNG
CSF2
TNF
CTLA4
IKZF3
MAF
IL-10
LLRC32
STAT5A
IKZF1
PRDM1
SOCS3
H
TH17-IL-22+/IFNγ+ vs TH17-IL-10+ at Day5
I
IKZF1
IKZF3
IKZF4
Relative expression
ns
****
***
**
Day0 Day5
TH17 IL-22+/IFNγ+
TH17 IL-10+
J
IL-22 signature
IL-10 signature
module score
UMAP2
UMAP1

program upon activation (Fig. S3F) By contrast, TH17-IL-10+ clones expressed significantly higher mRNA levels of *IL10, MAF* and other immune-modulatory genes such as *LRRC32* (which encodes for GARP), *PRDM1* (BLIMP-1), *CTLA4*, and *IKZF3* (Aiolos) (Fig. 2G, H). While similar inflammation-related pathways were significantly enriched at both time points, the fold change was slightly higher at day 0 than at day 5 (Fig. 2G, H and Fig. S3C).

IkZF transcription factors are differentially expressed in human memory TH17 cell subsets

The Ikaros Zinc Finger (IkZF) TF family members have similar DNA binding sites, and most have been linked with TH17 development. Consequently, we evaluated the expression of IkZF factors, including IKZF1, IKZF2, IKZF3, and IKZF4, within our RNA-seq dataset. We found that IKZF1 expression was significantly increased in the TH17-IL-22+/IFNγ+ subset at day 0 but not at day 5 (Fig. 2G, H), while IKZF3 was significantly increased in the TH17-IL-10+ subset both at day 0 and day 5 and, IKZF4 expression was increased in the TH17-IL-22+/IFNγ+ subset at day 5 (Fig. 2G, H) whereas IKZF2 was found not to be differentially expressed. Differential expression of IKZF3 and IKZF4 at day 5 was validated by qPCR (Fig. 2I). These findings were largely consistent with changes in chromatin accessibility as the IKZF3 locus (day 5) was more accessible in TH17-IL-10+ subset, while the IKZF4 locus (day 0 and day 5) was more accessible in the TH17-IL-22+/IFNγ+ (Fig. S4A, B).

To assess the correspondence between these TH17 subclones and the TH17 subsets identified in publicly available single-cell RNA-sequencing data derived from patients with allergic asthmatic patients [7], we performed a UMAP projection of module scores derived from the bulk RNA-seq data of TH17-IL-22+/IFNγ+ and TH17-IL-10+ clones (Fig. 2J, S4C, D).

The module scores were calculated based on the expression of genes found to be part of IL-22 and IL-10 expression signatures (Supplementary Tables 4, and 5 for gene lists). The UMAP projection demonstrated that the gene expression profiles of our TH17 subclones aligned with the corresponding TH17 subsets identified from allergic asthma patient samples, further supporting the existence of functionally distinct TH17 populations. Notably, the IL-10-expressing TH17 cells were found to express known transcription factors such as MAF and Aiolos, while the IL-22/IFNγ-expressing TH17 cells showed distinct expression patterns. This differential expression pattern of IKZF transcription factors across the TH17 subsets suggests their potential role in regulating the balance between pro-inflammatory (IL-22/IFNγ) and immunomodulatory (IL-10) cytokine expression.

Targeting IKZF1/3 with lenalidomide shifts human memory TH17 cells towards a pro-inflammatory phenotype

To investigate whether Ikaros TFs regulate the transcriptional phenotype of TH17 subsets, we specifically depleted Ikaros and Aiolos in memory TH17 cells using lenalidomide, which induces proteasomal degradation of these transcription factors via the E3 ligase Cereblon [33, 34]. Memory TH17 cells were activated with anti-CD3 and anti-CD28 for 4 days in the presence of different concentrations of lenalidomide or DMSO (Fig. 3A).

Increasing concentrations of lenalidomide led to a progressive decrease in Aiolos and Ikaros protein levels, corresponding to the genes IKZF3 and IKZF1, respectively, while expression of Eos protein, corresponding to the gene IKZF4, was concomitantly increased (Fig. 3B and S5A). Gene expression analysis of the three transcription factors (TFs) demonstrated a distinct regulatory response to lenalidomide treatment. Specifically, IKZF3 expression was downregulated at the lowest dose of lenalidomide, whereas both IKZF1 and IKZF4 were upregulated following exposure to 1 μM lenalidomide (Fig. S5C). This degradation pattern was accompanied by a dose-dependent increase in the expression of IFNγ, and IL-22, while IL-10 expression was reduced (Fig. 3C, D). Lenalidomide treatment increased total IL-17A and IL-17F protein in culture supernatants (Fig. S5B) but decreased the percentage of IL-17–expressing cells detected by intracellular flow cytometry (Fig. 3D, E). Additionally, qPCR analysis showed upregulation of IL-22, IFNγ, TNFα, IL-17F, IL-21, and IL-2 mRNA in response to 0.1 and 1 μM lenalidomide (Fig. S5C). Collectively, these findings demonstrate that lenalidomide-mediated IkZF degradation alters the transcriptional profile of TH17 cells, shifting cytokine expression toward a pro-inflammatory program.

Next, we investigated the temporal link between lenalidomide-induced effects on cytokine expression and the degradation of Aiolos and Ikaros by following the expression of IKZF TF family members and cytokines in memory TH17 cells over time. Lenalidomide treatment caused progressive degradation of Ikaros and Aiolos (days 1–3), with Eos expression increasing at later time points (day 4) (Fig.S6A). Intracellular flow cytometry analysis revealed that lenalidomide treatment decreased the percentage of IL-10– and IL-17–expressing cells at all examined time points, while the frequency of IL-22– and IFNγ–expressing cells increased, peaking on day 4 (Fig. 3E). In contrast, qPCR analysis of mRNA levels showed upregulation of all measured effector cytokines (IL-22, IFNγ, TNFα, IL-17F, IL-21, and IL-2) in lenalidomide-treated cells over time, with the exception of IL-10 mRNA, which was downregulated (Fig. S6B).

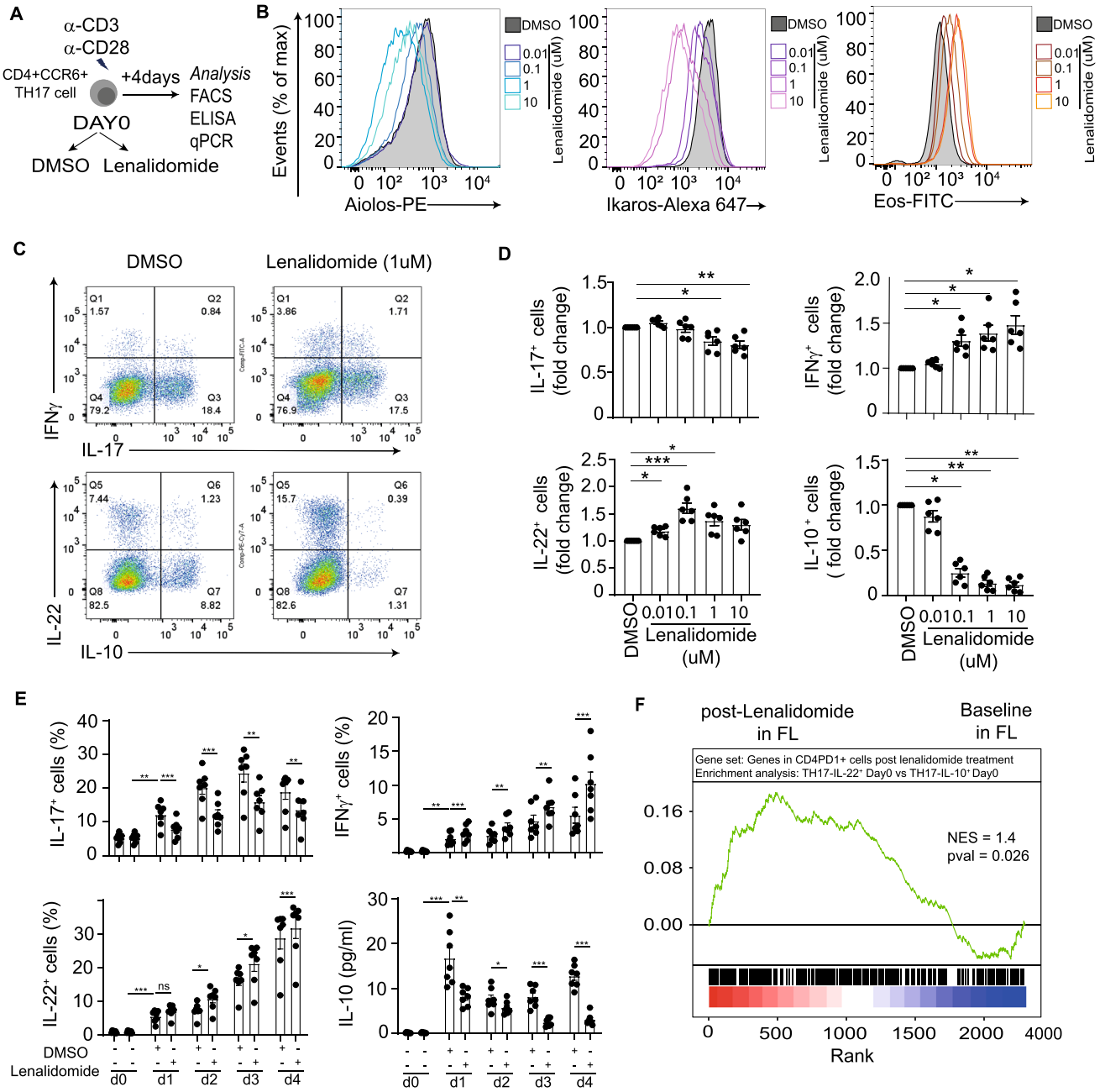

Fig. 3 Lenalidomide-Induced Degradation of Aiolos/Ikaros Modulates Inflammatory Versus IL-10 Cytokine Production by TH17 Cells. **A** Schematic of the experimental workflow: human memory TH17 cells were activated with anti-CD3 and CD28 for 4 days in the presence of DMSO or lenalidomide at different concentrations. **B** Histograms showing Aiolos, Ikaros, and Eos levels in memory TH17 cells activated with anti-CD3 and CD28 and treated with lenalidomide (0.01, 0.1, 1, or 10 μM) or DMSO for 4 days; one representative donor. **C-D** Representative FACS plot of intracellular cytokine expression in human memory TH17 cells treated with 1 μM lenalidomide compared to DMSO control as in (**A**). **D** Fold change of intracellular cytokine expression in human memory TH17 cells treated with lenalidomide compared to DMSO control after PMA/ionomycin restimulation. **E** Human memory TH17 cells were cultured for 4 days in the presence of DMSO or lenalidomide (1 μM), with the compounds added at different time points (day 1, 2, 3, and 4) during the culture period. Intracellular cytokine expression was measured after 4 hours of PMA/ionomycin restimulation. Each symbol represents an individual donor ($n=6$); mean±s.e.m. *$P<0.05$, **$P<0.01$, ***$P<0.001$, and ****$P<0.0001$ (one-way ANOVA). **F** GSEA-enrichment plots comparing the gene signature of lenalidomide-treated (day 7 vs day 0) CD4+ PD1+ cells from follicular lymphoma patients (Menard, Rossille et al. 2021) with the differentially expressed genes in TH17-IL-22$^+$ versus TH17-IL-10$^+$ cells

Together, these temporal data demonstrate that lenalidomide-mediated IkZF degradation progressively shifts the TH17 cytokine program from IL-10 toward IL-22 and IFNγ production.

To further validate the potential of lenalidomide in modulating cytokine expression pattern by TH17 cells, we analyzed publicly available RNA datasets derived from PBMC of follicular lymphoma patients before and after lenalidomide treatment [35]. Intriguingly, we found that TH17-IL-22^{+} clonal signatures were more strongly associated with lenalidomide treatment versus TH17-IL-10^{+} signatures, suggesting that lenalidomide may drive the transition of TH17 cells from an IL-10-producing phenotype to a more inflammatory, IL-22/IFNγ-producing state in a clinical setting (Fig. 3F). Additionally, corroborating our GSEA analysis which indicated that TH17 inflammatory cells have a higher IL-2-induced gene expression signature (Fig. S6C), we observed that lenalidomide treatment in TH17 cells led to an increase in phospho-STAT5 levels (Fig. S6D). This increase was concurrent with the rise in IL-2. In contrast with IL-17, STAT5 has been shown to play are role in enhancing IL-22 [36] and IFNγ expression [37]. Thus, our data suggest that, following the degradation of Aiolos and Ikaros, there is a transition towards a more pro-inflammatory phenotype.

Collectively, our transcriptomic analysis demonstrates that Aiolos and Ikaros play important roles in regulating inflammatory gene expression in human memory TH17 cells, with their degradation resulting in a marked shift towards a pro-inflammatory phenotype, characterized by the up-regulation of genes involved in inflammatory response, cytokine signaling, and T cell activation, and the downregulation of genes associated with IL-10 signaling and anti-inflammatory response.

Distinct roles of Aiolos, Ikaros, and Eos in regulating cytokine expression in human memory TH17 cells

To investigate the specific contribution of these transcription factors in TH17 cells, we employed CRISPR-Cas9 to delete IKZF1 and IKZF3 (Fig.S4A). While we initially attempted IKZF4 knockout, we were unable to confirm protein-level downregulation due to the substantially lower basal expression of Eos compared to Ikaros and Aiolos (Fig. 2I); therefore, we pursued lentiviral overexpression to assess IKZF4 function (see below). CRISPR-KO for IKZF1 was approximately 20% efficient (Fig. 4B, and S7A), whereas CRISPR-mediated KO of IKZF3 was about 80% efficient (Fig. 4B, and S7B). We found that significantly fewer Ikaros- cells expressed IFNγ, IL-22 and IL-17 (flow cytometry) as compared to both control conditions (Fig. 4C, and Fig. S7C). IKZF1-KO did not affect IL-10 expression (Fig. 4C). Aiolos- cells expressed significantly less IL-10 and more IL-22 when compared to both control conditions (Fig. 4D, and S7D). Suggesting that Aiolos, but not Ikaros, positively regulates IL-10. Finally, the inhibition of either Ikaros or Aiolos led to an increase in Eos (IKZF4) expression, suggesting a potential compensatory relationship between these transcription factors. We then employed a lentivirus-based overexpression (o/e) approach to address the role for Eos in memory TH17 cytokine regulation (Fig. 4E). We found that Eos was overexpressed in ~25% of transduced cells (Fig. 4F, G) and overexpression did not affect transcript levels of IKZF1 and IKZF3 mRNA (Fig. S7E). Strikingly, Eos o/e significantly reduced IL-10 expression (flow cytometry, mRNA and in supernatant, Fig. 4H, and S7E, F) while inducing several pro-inflammatory cytokines such as IL-17A/F, IFNγ, TNFa and GM-CSF, IL-13, IL-21, MIP1a (mRNA and in supernatant) and IL-22 in some conditions. These results suggest that Eos positively regulates pro-inflammatory cytokines such as IL-17, IFNγ and IL-22, while inhibiting IL-10 expression. These results suggest that Eos positively regulates pro-inflammatory cytokines such as IL-17, IFNγ and IL-22, while inhibiting IL-10 expression. Taken together, these findings suggest that IkZF TFs play important roles in TH17 function with

Fig. 4 Specific contribution of Aiolos, Ikaros and Eos to modulate memory T_H17 cell plasticity. Human memory TH17 cells were activated with anti-CD2, anti-CD3 and anti-CD28 for 24 hours prior electroporation with non-targeting gRNA (CTRL), gRNAs for CRISPR-Cas9-dependent IKZF1 or IKZF3 knock-out (KO) (A-B-C-D). IKZF1, IKZF3, and IKZF4 encode Ikaros, Aiolos, and Eos, respectively. **A** Schematic representation of the workflow. **B** Intracellular staining of Aiolos and Ikaros in memory TH17 cells in CTRL, IKZF1 KO and IKZF3 KO, 5 days after electroporation. Numbers in quadrants indicate percent cells, representative donor (right), frequency of Aiolos+ and Ikaros+ in memory TH17 cells comparing Q1, Q2 and Q3 quadrants for CTRL, IKZF1 KO and IKZF3 KO (left), 5 days after electroporation. **C** Frequency of cytokines in memory TH17 cells in IKZF1 KO, gated on Aiolos+Ikaros- (Q1 in IKZF1 KO, Fig. 4B) and Aiolos+Ikaros+ (Q2 in IKZF1 KO, Fig. 4B), 5 days after electroporation and 4 hours of stimulation with PMA/Ionomycin. **D** Frequency of cytokines in memory TH17 cells in IKZF3 KO, gated on Aiolos-Ikaros+ (Q3 in IKZF3 KO, Fig. 4B) and Aiolos+Ikaros+ (Q2 in IKZF3 KO, Fig. 4B), 5 days after electroporation and 4 hours of restimulation with PMA/Ionomycin. Each symbol represents an individual memory TH17 donor, $n=6$; mean±s.e.m. $*P<0.05$, $**P<0.01$, $***P<0.001$ and $****P<0.0001$ (paired t-test). **E-F-G-H** Memory TH17 cells were activated as in (**A**) prior lentivirus transduction for Eos overexpression with pLV-Puro-SFFV-TagBFP2-T2A-hIKZF4/HA or control lentivirus pLV-Puro-SFFV-TagBFP2 (CTRL). **E** Schematic representation of the workflow. **F** Representative flow cytometry analysis (right) of BFP2- (light grey) and BFP2+ TH17 cells and BFP2+ TH17 cells (left) in Eos overexpression (o/e, orange) and CTRL (dark grey) conditions. **G** Representative Mean Fluorescent Intensity (MFI) histogram (right) or cumulative data (left) of Eos expression in CTRL BFP2+, BFP2- and BFP2+ in Eos o/e. **H** Frequency of cytokines in memory TH17 cells as in (**D-E**). Each symbol represents an individual memory TH17 donor, $n=6$; mean±s.e.m. $*P<0.05$, $**P<0.01$, $***P<0.001$ and $****P<0.0001$ (one-way ANOVA)

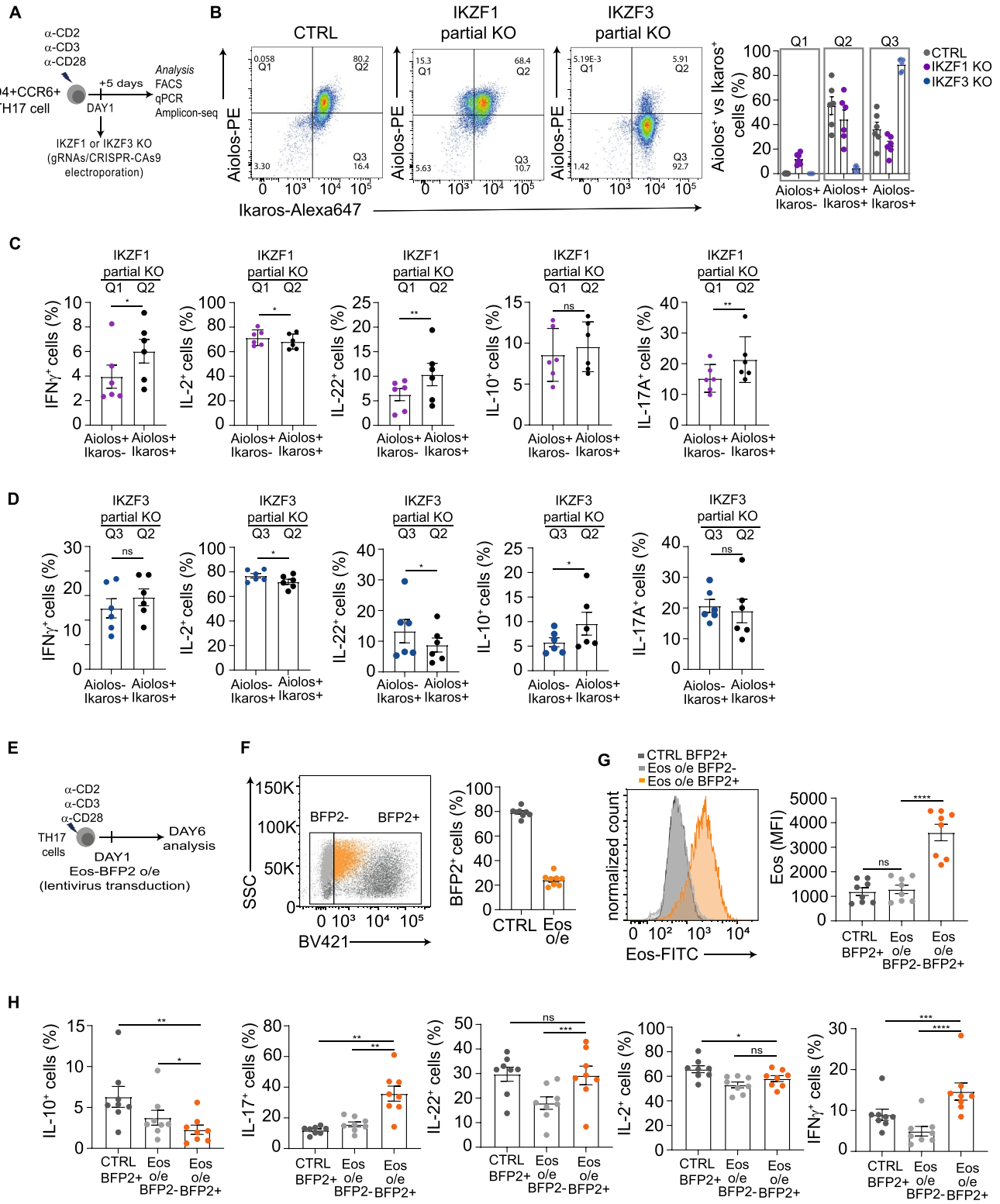

each family member having distinct effects on cytokine profiles. Specifically, Aiolos appears to positively regulate IL-10 expression during TH17 cell activation, while Eos promotes pro-inflammatory cytokine expression including IL-22, IL-17 and IFNγ. The role of Ikaros appears more complex, with effects on multiple cytokines but less pronounced impact on IL-10 specifically.

These results suggest that Eos positively regulates pro-inflammatory cytokines such as IL-17, IFNγ and IL-22, while inhibiting IL-10 expression. Taken together, these

findings suggest that IkZF TFs play important roles in TH17 function with each family member having distinct effects on cytokine profiles. Specifically, Aiolos appears to positively regulate IL-10 expression during TH17 cell activation, while Eos promotes pro-inflammatory cytokine expression including IL-22, IL-17 and IFNγ. The role of Ikaros appears more complex, with effects on multiple cytokines but less pronounced impact on IL-10 specifically.

Lenalidomide-mediated TH17 reprogramming occurs independently of IL-2 signaling pathways

To determine whether the cytokine changes observed following IKZF3/Aiolos deletion or lenalidomide treatment were direct transcriptional effects or mediated indirectly through IL-2, we investigated IL-2's role in TH17 cytokine regulation. Since Aiolos is known to repress IL-2 expression, its deletion or degradation could potentially alter TH17 cytokine profiles by changing IL-2 levels rather than through direct cytokine gene regulation.

We found that TH17-IL-22+ clones, in comparison to TH17-IL-10+ clones, produce substantially more IL-2 at RNA and protein level as well as display an IL-2-induced STAT5 gene signature (Fig. 2G, H; and S5B and S6C, D). To delineate the influence of IL-2 signaling on cytokine expression in polyclonal TH17 cells, we employed neutralizing antibodies against IL-2 and IL-2Rβ, alongside the addition of recombinant human IL-2 (Fig. 5A). Intracellular flow cytometry analysis revealed that neutralizing IL-2 led to a significant reduction in IL-10 expression, whereas the levels of IFNγ and IL-17 remained unaffected (Fig. 5B). Recombinant IL-2 strongly increased IL-10 production with no discernible impact on IFNγ, IL-22 or IL-17 (Fig. 5B and S8A). Importantly, lenalidomide effects on cytokine expression occurred independently of IL-2 levels. Lenalidomide inhibited IL-10 and enhanced IL-22 expression equally in the presence or absence of IL-2 (Fig. 5B, C), demonstrating that IkZF transcription factor regulation of TH17 subsets operates through direct mechanisms rather than indirect IL-2-mediated effects.

In this experiment, lenalidomide did not alter IL-22 expression either in the presence or absence of IL-2 as measured by ICS (Fig. 5B). Lenalidomide did enhance IL-22 expression by qPCR and increase IL-22 measured in the supernatant, but again this was not affected by the presence or absence of IL-2 (Fig. 5C). We found that lenalidomide did inhibit IL-10 expression by ICS and qPCR but again this was equally true in the presence or absence of IL-2. Neutralizing endogenous IL-2 increased Eos expression in TH17 cells, implying a repressive effect of IL-2 on Eos. Conversely, exogenous IL-2 elevated all three IkZF TFs proteins (Fig. S8B). These findings demonstrate that IkZF transcription factors directly regulate TH17 cytokine expression rather than acting indirectly through IL-2-mediated pathways.

Lenalidomide modulates TH17 inflammatory signatures in follicular lymphoma patients

To validate the clinical relevance of these observations, single-cell RNA sequencing (scRNA-seq) was performed on peripheral blood mononuclear cells (PBMCs) from three patients in the GALEN clinical trial (#NCT01582776) before treatment (D0) and after one week of lenalidomide monotherapy (D7). T cells were isolated from cryopreserved PBMC samples and subject to single cell RNAseq analysis. From 28,946 CD4+ T cells (excluding regulatory T cells) (Fig. S9A), dimensional reduction and clustering revealed seven distinct clusters. Due to the small fraction of TH17 cells within the CD4+ population, established TH17 signature markers including RORA, RORC, ICOS, AHR, IL17A, IL17F, CCL20, CTSH, IL22, and CCR6 were utilized for identification, revealing that cluster 7 exhibited characteristic TH17 features (Fig. S9B).

Subsequent sub-clustering of 5630 TH17-like cells yielded eight clusters (Fig. S10A), from which five clusters (totaling 1990 cells) were selected based on expression of canonical TH17 markers and further classified into C1 (classic TH17) and C2 (inflammatory TH17) subsets (Fig. S10B,C). Cluster annotation was validated through transcriptional similarity to reference TH17 datasets (Fig. 6A). Using TH17-IL-22+/IFNγ+ and TH17-IL-10+ clonal signatures from bulk RNA-seq data, all TH17 cells segregated into two distinct populations: C1 demonstrated high IL-10 signature positivity while C2 showed IL-22 signature enrichment, confirming the existence of functionally distinct TH17 subsets in follicular lymphoma patients (Fig. 6B).

Following lenalidomide treatment, differential gene expression analysis (P value <0.05, fold change cutoff = 1) revealed upregulation of proinflammatory genes (IFNγ, TNF) in the C1 cluster and effector molecules (GNLY, NKG7, GZMH) in the C2 cluster (Fig. 6C). Pathway enrichment analysis confirmed activation of inflammatory signatures, including interferon and IL-2/STAT5 pathways, in TH17 cells post-lenalidomide treatment (Fig. 6D). These findings provide clinical validation that lenalidomide promotes inflammatory responses in TH17 cells from follicular lymphoma patients, corroborating the in vitro and ex vivo experimental data.

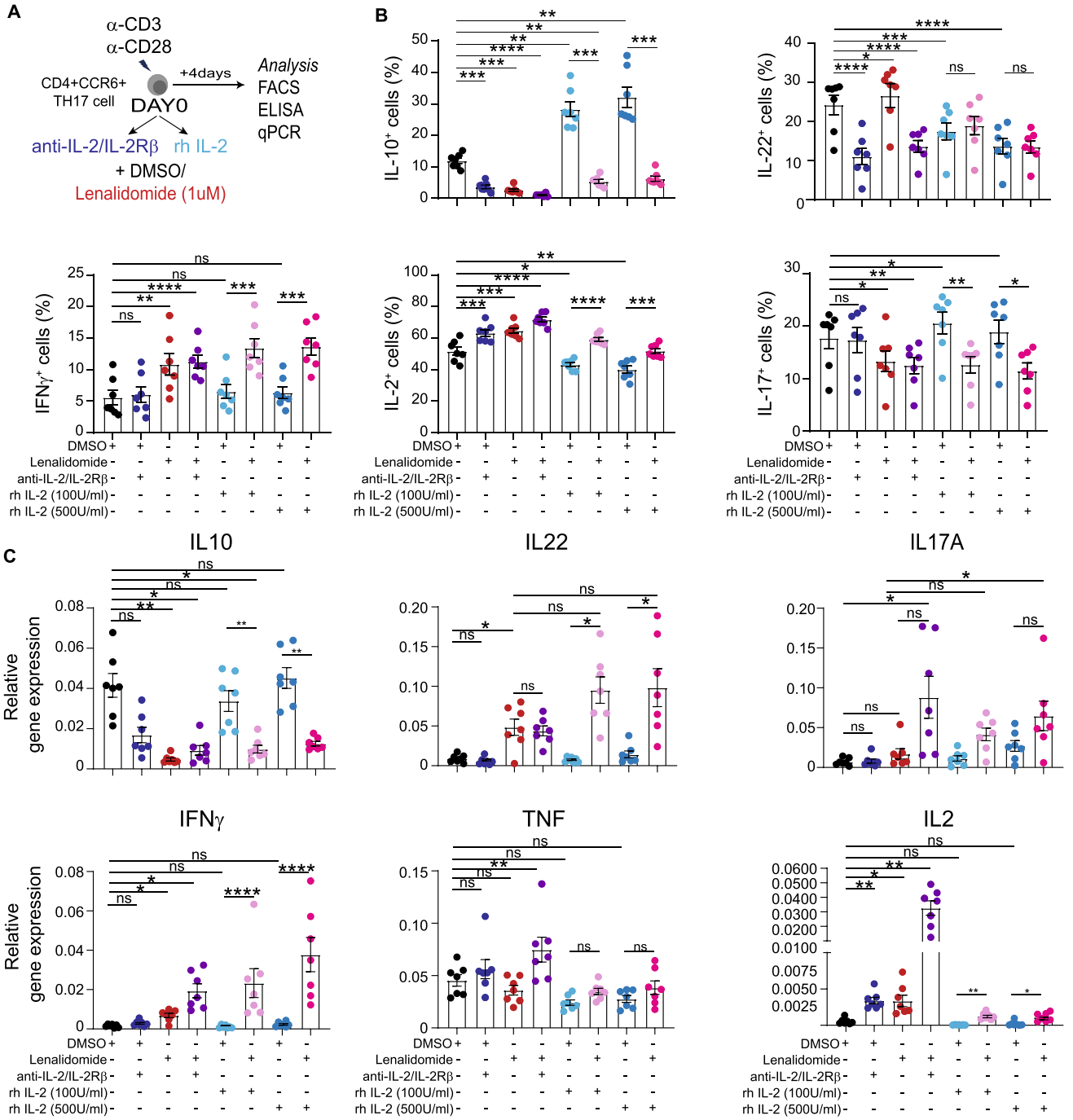

Fig. 5 Lenalidomide Enhances IL-22/IFNγ and Inhibits IL-10 Independent of IL-2. **A** Schematic representation of the workflow: human memory TH17 cells were isolated from healthy donors and were activated with anti-CD3 and anti-CD28 for 4 days in presence of blocking antibody against IL-2/IL-2Rβ or recombinant human (rh) IL-2 (100 U/ml or 500 U/ml) in presence of DMSO or lenalidomide (1uM). **B** Frequency of cytokines in memory TH17 cells 4 days after activation and 4 hours after PMA/ionomycin restimulation. **C** Relative gene expression of cytokines in memory TH17 cells, 4 days after activation. Each symbol represents an individual memory TH17 donor, $n=6$; mean ± s.e.m. $*P<0.05$, $**P<0.01$, $***P<0.001$ and $****P<0.0001$ (one-way ANOVA)

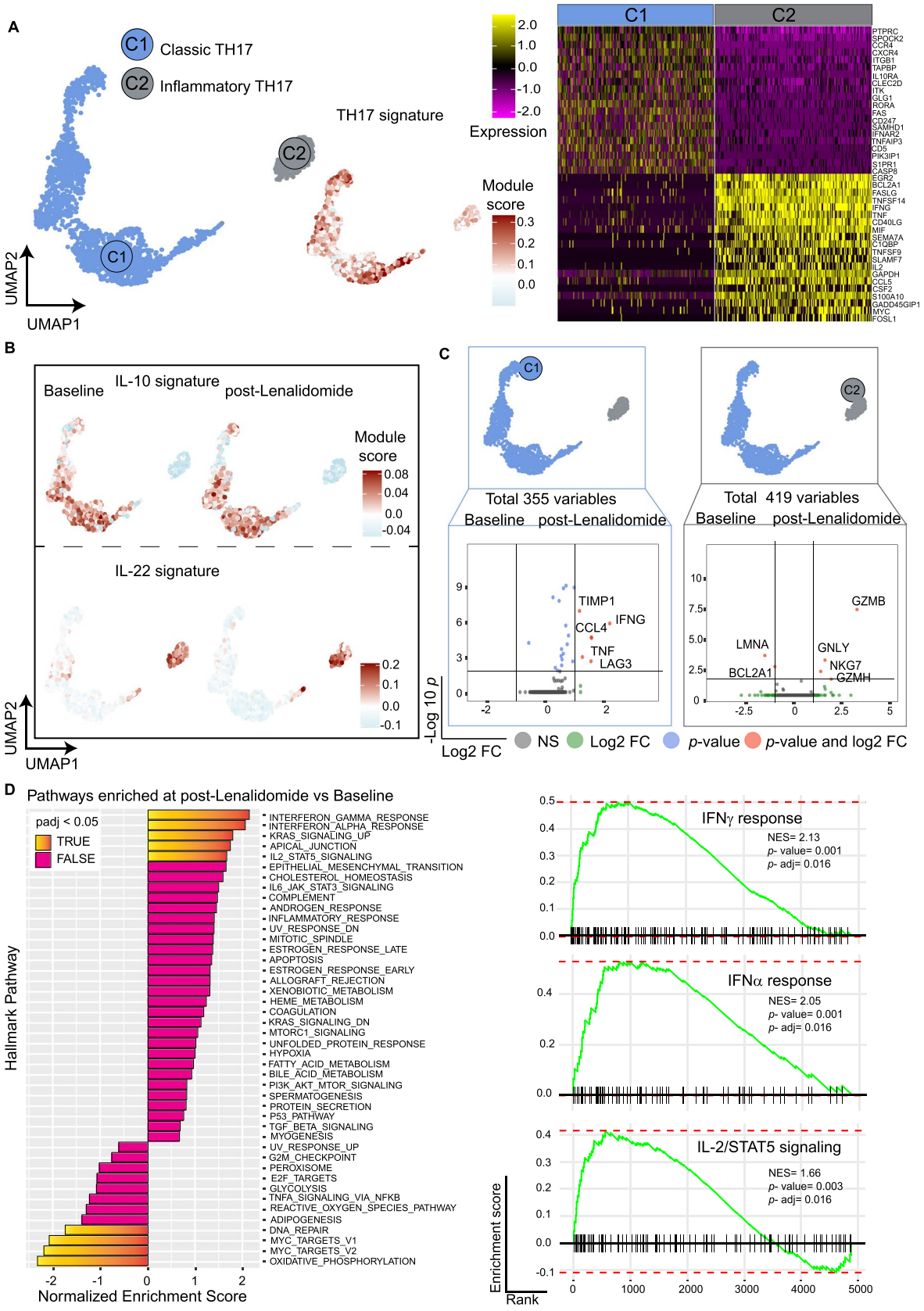
A
C1 Classic TH17
C2 Inflammatory TH17
TH17 signature
Expression
Module score
UMAP2
UMAP1
C1
C2
B
Baseline
IL-10 signature
post-Lenalidomide
IL-22 signature
C
Total 355 variables
Total 419 variables
Baseline post-Lenalidomide
TIMP1
IFNG
CCL4
TNF
LAG3
GZMB
LMNA
GNLY
NKG7
BCL2A1
GZMH
-Log 10 p
Log2 FC
NS
Log2 FC
p-value
p-value and log2 FC
D
Pathways enriched at post-Lenalidomide vs Baseline
padj < 0.05
TRUE
FALSE
Hallmark Pathway
Normalized Enrichment Score
IFNγ response
NES= 2.13
p- value= 0.001
p- adj= 0.016
IFNα response
NES= 2.05
p- value= 0.001
p- adj= 0.016
IL-2/STAT5 signaling
NES= 1.66
p- value= 0.003
p- adj= 0.016
Enrichment score
Rank

Fig. 6 Lenalidomide Promotes Inflammatory Responses in TH17 Cells from Follicular Lymphoma Patients in vivo. **A** UMAP visualization of 1990 TH17 cells from peripheral blood of follicular lymphoma patients before and after lenalidomide treatment, clustered into two groups: C1 (classic TH17) and C2 (inflammatory TH17). Small UMAP (right) confirms all cells express TH17 signatures. Heatmap shows expression of TH17 signature genes across both clusters, with module scores indicating TH17 signature expression levels. **B** UMAP projections showing IL-10 and IL-22 clonal signatures at Day 0 (baseline) and Day 7 (post-lenalidomide) treatment. Module scores represent the expression levels of IL-10+ regulatory versus IL-22+ inflammatory gene signatures across the TH17 cell populations. **C** Volcano plots showing differentially expressed genes between Day 0 (baseline) and Day 7 (post-lenalidomide) treatment for C1 (classic TH17, left) and C2 (inflammatory TH17, right) clusters. Notable upregulated genes include TIMP1, CCL4, IFNG, TNF, and LAG3 in C1, and GZMB, GZMH, GNLY and NKG7 in C2. **D** Pathway enrichment analysis comparing Day 7 (post-lenalidomide) versus Day 0 (baseline) conditions. Left panel shows hallmark pathways with normalized enrichment scores; right panels show gene set enrichment analysis (GSEA) plots for interferon-γ response, interferon-α response, and IL-2/STAT5 signaling pathways

Discussion

Human TH17 cells exhibit functional heterogeneity through differential cytokine production programs that regulate both immune activation and tissue homeostasis. Originally defined by their capacity to produce IL-17, TH17 cells have emerged as critical mediators of mucosal immunity and inflammatory disease [2, 11], with distinct subsets exhibiting either pathogenic pro-inflammatory or tissue-protective regulatory functions [13, 14]. This study addresses the clinical question of how TH17 cell functional states can be therapeutically modulated, with specific focus on identifying molecular mechanisms that govern transitions between regulatory and inflammatory phenotypes in humans. While TH17 cell plasticity has been extensively characterized in murine models, the transcriptional networks controlling human TH17 subset specification remain incompletely understood, limiting therapeutic applications.

The present investigation demonstrates differential expression of IkZF transcription factors across human TH17 subsets through comprehensive transcriptomic and epigenetic analyses of clonally expanded memory TH17 cells. Two functionally distinct subsets were characterized: TH17-IL-10+ cells and TH17-IL-22+/IFNγ+ cells displaying contrasting cytokine profiles. TH17-IL-10+ cells expressed regulatory-associated markers including CTLA-4 and GARP while maintaining IL-17 production, defining a non-inflammatory TH17 subset distinct from the pro-inflammatory TH17-IL-22+/IFNγ+ population. Notably, both subsets exhibited reduced IL-17 expression upon activation, reflecting TH17 lineage plasticity whereby commitment to alternative effector programs (Th1-like or regulatory) constrains IL-17 expression through mutually antagonistic transcriptional networks [11, 19, 38]. Most significantly, IKZF3 (Aiolos) demonstrated robust enrichment in TH17-IL-10+ cells at both resting and activated states, representing the strongest differential expression signal observed across all conditions tested. In contrast, IKZF4 (Eos) showed selective upregulation in TH17-IL-22+/IFNγ+ cells following activation, while IKZF1 (Ikaros) exhibited more modest subset-specific differences.

Functional validation through genetic knockout approaches and pharmacological degradation studies established that manipulation of IkZF expression directly influences TH17 cytokine production profiles. CRISPR-mediated knockout of IKZF3 resulted in reduced IL-10 expression and enhanced IL-22 production, while lentiviral overexpression of IKZF4 promoted inflammatory cytokine production including IL-17, IFNγ, and IL-22 while suppressing IL-10. These findings provide direct evidence that IkZF transcription factors contribute to the regulation of human TH17 functional states, extending previous murine studies that identified Aiolos as a regulator of IL-2 and IL-17 expression [26]. Based on these findings and consistent with mouse studies showing Eos promotes effector cytokine production [39], we predict that Eos removal would attenuate IL-22 and IFNγ production in TH17-IL-22+/IFNγ+ cells, though this remains to be experimentally validated.

Lenalidomide was employed as a pharmacological tool due to its established mechanism of degrading IKZF1 and IKZF3 through cereblon-mediated proteasomal targeting [33, 34], providing a clinically relevant approach to test IkZF function in TH17 cells. Incubation of memory TH17 cells with increasing concentrations of lenalidomide resulted in progressive degradation of Aiolos and Ikaros proteins while concomitantly increasing Eos expression. This protein-level modulation was accompanied by dose-dependent increases in IFNγ and IL-22 expression and reduced IL-10 production. Importantly, lenalidomide-mediated changes in TH17 cytokine expression occurred independently of IL-2 availability, indicating that IkZF-mediated regulation represents a distinct pathway from traditional cytokine-driven mechanisms.

Single-cell RNA sequencing analysis of PBMCs from follicular lymphoma patients receiving lenalidomide therapy provided clinical validation of the in vitro mechanistic findings. Despite the limited sample size, differential gene expression analysis revealed upregulation of proinflammatory genes including IFNγ and TNF in classic TH17 cells, and effector-related genes such as GNLY, NKG7, and GZMH in inflammatory TH17 cells following lenalidomide administration. Pathway enrichment analysis confirmed activation of inflammatory signatures, including interferon and IL-2/STAT5 pathways in TH17 cells following lenalidomide treatment, demonstrating that pharmacological IkZF modulation can reprogram TH17 responses in patients.

While our data demonstrate that lenalidomide-mediated IkZF degradation alters TH17 cytokine production profiles, we acknowledge that our current experimental design does not definitively distinguish between direct transcriptional control through IkZF function versus indirect effects mediated by autocrine or paracrine signaling pathways. Specifically, the discordance between intracellular cytokine staining and bulk measurements (qPCR, ELISA) under conditions of IL-2 neutralization suggests that feedback mechanisms and secreted cytokine signaling may contribute substantially to the observed phenotype. Future studies employing conditional deletion of IKZF factors in mouse Th17 cells and targeted pharmacological degradation approaches would be necessary to definitively establish whether IkZF proteins exert direct transcriptional control over cytokine genes or operate primarily through modulation of cytokine-driven signaling networks.

These findings may potentially highlight a dual role for inflammatory TH17 activation, contributing to lenalidomide-induced anti-tumor immunity through Aiolos degradation, while also possibly driving adverse effects, such as psoriasis exacerbation [40, 41] and graft-versus-host disease [42, 43], could stem from increased pro-inflammatory TH17 responses. Our TH17-IL-22+ signatures aligned with distinct TH17 populations in allergic asthma patients (Fig. 2J), consistent with the established role of IL-17/IL-22-producing Th17 cells in allergic airway inflammation [44], and it would be of interest to determine whether similar inflammatory TH17 signatures are enriched in chronic inflammatory disorders such ng multiple sclerosis and rheumatoid arthritis.

While effect sizes were moderate, the consistent directional changes across multiple experimental systems support the biological significance of IkZF-mediated effects on TH17 function. The clinical validation, though limited by sample size, provides important proof-of-concept evidence for lenalidomide's effects on TH17 cell signatures in humans. Future studies should validate these findings across larger patient cohorts and investigate whether IkZF expression patterns can serve as predictive biomarkers for lenalidomide responses and adverse events.

In conclusion, we show differential expression of IkZF transcription factors across human TH17 cell subsets and demonstrate that lenalidomide-mediated IkZF degradation can alter TH17 cytokine production profiles. The findings provide mechanistic insights into human TH17 subset regulation and suggest that IkZF proteins may represent targets for modulating TH17 function in therapeutic contexts. These results advance understanding of the molecular mechanisms governing human TH17 cell heterogeneity and provide a foundation for developing targeted approaches to manipulate TH17 responses in cancer and autoimmune diseases.

Materials and methods

Sex as biological variable

Sex was not considered as a biological variable in this study. Both male and female samples were included from healthy donors and follicular lymphoma patients, but the study was not designed or powered to detect sex-specific differences in TH17 cell characteristics or responses to lenalidomide treatment.

Blood samples and cell sorting

Peripheral blood mononuclear cells were isolated from fresh blood using Sepmate and Lymphoprep (STEMCELL Technologies) density gradient centrifugation and samples were enriched for CD4 + CCR6 + CXCR3- TH17 cells to an average purity of 95% using EasySep™ Human TH17 Cell Enrichment Kit II (STEMCELL#17862), referred here as "bulk TH17 cells". Viable IL-17-producing bulk TH17 cells were sorted by flow cytometry using the IL-17 cytokine secretion assay (Miltenyi Biotec#130–094–536) following 3 h of stimulation with phorbol 12-myristate 13-acetate (PMA) (0.2 µM) and ionomycin (1 µg/ml) (both from Sigma-Aldrich), according to the manufacturer's instructions. Single cell sorting was performed using a FACSAria III device (BD Biosciences).

Human TH17 clone culture

Human TH17 clone cells were cultured in RPMI-1640 medium supplemented with 1% (v/v) glutaMAX-I, 25 mM HEPES, 1% (v/v) non-essential amino acids, 1 mM sodium pyruvate, 50 µM β-mercaptoethanol, penicillin (50 U/ml), streptomycin (50 µg/ml) and 1% (v/v) kanamycin (all from Gibco, Life Technologies), plus 5% (v/v) heat-inactivated human serum (SIGMA-Aldrich#H3667) (called 'complete medium' here). 500 U/ml IL-2 (Thermofisher# PHC0026) was added to the culture medium for long-term cultures. Single TH17 cell clones were cell sorted in 384-well plates and underwent population expansion with allogeneic irradiated (50 Gy) feeder cells (2.5×10^4 cells per well) and phytohemagglutinin (1 µg/ml; Remel) in complete medium containing IL-2 (500 U/ml) which were seeded the day before. Where indicated, TH17 cells were stimulated with plate-bound anti-CD3 (0.5 µg/ml, clone: TR66) and anti-CD28 (0.5 µg/ml, clone: CD28.2, BD Biosciences). T cell clones were analyzed as previously described (Aschenbrenner et al., 2018). Briefly, T cell clones were analyzed at day 0 (resting state) and at day 5 (recently activated state - after stimulation for 48 h in plates coated with anti-CD3 and CD28 antibody, and additional 3 days of culture in

uncoated plates). Day 0 (resting) and day 5 (activated) T cell clones were stimulated for 5 h with Cell Stimulation Cocktail (plus protein transport inhibitors, eBioscience# 00–4975-03) (for protein analysis) or for 2 h with plate-bound anti-CD3 and anti-CD28 (for RNA and chromatin-accessibility analysis - RNA and ATAC-seq section in supplemental material).

Bulk TH17 cells were cultured in RPMI-1640 medium containing the following supplements: 1% (v/v) GlutaMAX-I, 1% (v/v) non-essential amino acids, 1 mM sodium pyruvate, 1% (v/v) L-glutamine, 50 U/mL penicillin and streptomycin and 10% heat-inactivated FBS (all from Gibco, life Technologies). Isolated TH17 cells (EasySep Hu TH17 Cell Enrichment kit II STEMCELL#17862) were activated using the T Cell Activation/Expansion kit (Miltenyi #130–091–441). To this end 1×10^6 cells/mL were activated at bead to cell ratio of 1:5 and $0{,}5 \times 10^5$ cells per well were seeded into round-bottom tissue culture treated 96-well plates for four days when treated with Lenalidomide at a final concentration of 1uM (Sigma-Aldrich#SML2283) or DMSO (SIGMA-Aldrich#D2438), otherwise specified. Alternatively, Lenalidomide or DMSO were added at different time points after activation as specified in the figures. For phospho-STAT analysis, bulk TH17 cells were isolated from 2 or more donors as described above without or with 1 or 10 µM lenalidomide for 4 days. For IL-2 neutralization experiments, $0{,}5 \times 10^5$ cells per well were incubated with the antibody against IL2 and IL-2Rβ at a final concentration of 10 µg/ml for 30 minutes prior activation and Lenalidomide or DMSO addition. Recombinant human (rh) IL-2 was added at a final concentration of 100 U/ml or 500 U/ml and time of cell activation in presence of Lenalidomide (1uM) or DMSO, only when specified in the figures. For cell transfection and transduction, 2×10^5 TH17 cells were activated with anti-CD2, CD3 and CD28 antibody at bead to cell ratio of 1:2 in a 96 well plate for 24 hours (see next sections).

Table 1 sgRNA & Oligo list

Target	sgRNA1	sgRNA2
IKZF1	U*C*A*UCUGGAGUAUCGCU UAC + modified scaffold	C*G*A*GG ACCUCUCC ACCACCU + modified scaffold
IKZF3	U*G*C*GGAACUGAAAAGCA CUC + modified scaffold	G*U*U*UU AAAGUCAG AACCCAU + modified scaffold
Oligo	Sequence	
Neon enhancer v2	TTATTAGGATATTTTTATTTTTTATTTTTTTTTT TTTTTTTTGGATAATTATTATTTTATTATTTATT TTTTTTTTATTAAATATTTTAAGGATA	

Cell transfections

Bulk TH17 cells were electroporated 24 hours after activation with ribonucleoprotein complexes (RNPs) using the 10 µL Neon transfection kit (MPK1096, Thermo Fisher). RNPs were prepared as follows; 5 µg of TrueCut Cas9 v2 (ThermoFisher#A36498), 1.2 µg of the selected sgRNA1 and sgRNA2 (TrueGuide Synthetic gRNA, Life Technologies) for each target gene (Table 1) were mixed and incubated for 15 minutes. In the meanwhile, cells were washed with PBS and resuspended in R buffer at a concentration of 5×10^7/mL. 2×10^5 cells were mixed with 1.2 µg of Neon enhancer v2 oligos (HPLC-purified) and electroporated with RNP complexes using the following settings: Voltage: 1600 V, width: 10 ms and pulse number: 3. After electroporation cells were incubated overnight in 0.5 mL of RPMI medium complemented with only 10% heat-inactivated FBS (Gibco#10500064) in a 24 well plate. The next day cells were collected, centrifuged at 300 *g* for 5 minutes, resuspended in 200 µL of complete growth medium and seeded in a 96 well plate. Transfected cells were analyzed five days after electroporation by flow cytometry and Amplicon-seq for editing efficiency.

Flow cytometry analysis

T lymphocytes were washed once with PBS and then stained with Fixable Viability Die eFluor780 (Thermo Fisher Scientific) for 10 minutes on ice to exclude dead cells from the analysis. For intracellular cytokine staining, cells were stimulated for 5 hours with CellStimulation Cocktail (eBioscience). Cells were then fixed and permeabilized with Cytofix/Cytoperm (BD Bioscience) according to manufacturer's instructions. The following conjugated antibodies were used for cytokine analysis: anti-IFNγ, anti-IL-2, anti-IL17, anti-IL-10, anti-IL-22; or transcription factor analysis: anti-Eos, anti-Aiolos, anti-Ikaros (Table 2 for antibody details). Stained cells were analyzed using a BD LSRFortessa (BD Biosciences), and flow cytometry data were analyzed with FlowJo software (Tree Star).

For phospho-STAT analysis, after 4 days in culture, TH17 cells were fixed in BD PhosFlow Fix Buffer I (BD Biosciences) at room temperature for 10–12 minutes, according to the manufacturer's protocol. Cells were centrifuged and washed once with cold PBS containing 2% FBS. Cells were then permeabilized by adding 200 µL ice-cold Perm Buffer III (BD Biosciences) per well and stored overnight at −20 °C. Cells were washed twice and stained with

Table 2 Flow cytometry antibody list

Antibodies	Source	Identifier
Fixable Viability Dye eFluor780	Thermo Fisher Scientific	65-0865-14
PE IL-17 Secretion Assay- detection kit	Miltenyi	130-094-536
		Clone
BV786 mouse anti-human IL-17	BD Bioscience	563745
PE-Cy7 mouse anti-human IL22	BD Bioscience	22URTI
FITC mouse anti-human IFNγ	BD Bioscience	B27
BV605 mouse anti-human IFNγ	BD Bioscience	B27
APC rat anti-human IL-10	BioLegend	JES3-9D7
BV421 rat anti-human IL-10	BioLegend	JES3-9D7
BV510 mouse anti-human IL-2	BD Bioscience	5344.111
BV421 mouse anti-human TNFa	BD Bioscience	MAb11
BV605 mouse anti-human CCR6	BD Bioscience	11A9
BV421 mouse anti-human CCR4	BD Bioscience	1G1
eFluor488 mouse anti-human CXCR3	BD Bioscience	1C6
Purified mouse anti-human EOS	BioLegend	W16032B
PE rat anti-human Aiolos	BioLegend	16D9C97
PE-CF594 mouse anti-human Ikaros	BD Bioscience	R32-1149
Alexa Fluor 647 mouse anti-human Ikaros	BD Bioscience	R32-1149
BV 421-mouse pSTAT3 (Tyr705)	BioLegend	13A3-1
pSTAT5 (Tyr694) Mouse IgG1 47/Stat5(pY694) PE	BD Bioscience	512567
Secondary antibody		
PE anti-rat IgG2a Antibody	BioLegend	MRG2a-83
FITC anti-rat IgG2a Antibody	BioLegend	MRG2a-83
Alexa 647 anti-rat IgG2a Antibody	BioLegend	MRG2a-83
Recombinant proteins and Blocking antibodies		
Recombinant human IL-2	gibco	PHC0027
Human IL-2 Antibody	R&D	MAB202-100
Human IL-2 R beta Antibody	R&D	MAB224-100

anti-phospho-specific antibodies and cell surface markers for 60 minutes at room temperature in the dark. Samples were washed twice and analyzed by flow cytometry on a FACS Fortessa instrument (BD Biosciences). The data were analyzed using FlowJo software. Live cells were gated based on FSC/SSC, and duplicates were removed using FSC-H vs FSC-A. Cells were then analyzed for phosphorylated STAT3 (pSTAT3) and pSTAT5 levels.

Cytokines quantification by Meso scale discovery (MSD)

25 uL of supernatant from the TH17 cells culture were used for cytokines quantification using the U-PLEX T Cell Combo (hu) SECTOR (MSD cat.n. K15093K-1), V-PLEX Human IL-2 Kit (MSD cat.n. K151QQD-1) and U-PLEX TH17 Combo 2 (hu) (MSD cat.n. K15076K) based on manufacturer's instructions.

Table 3 NGS primer list

Primer	Sequence
IKZF1_NGS_F	TCGTCGGCAGCGTCAGATG TGTATAAGAGACAGCCTCA TGCCACCCTCTCAAG
IKZF1_NGS_R	GTCTCGTGGGCTCGGAGAT GTGTATAAGAGACAGCTGG TGACCCACTTACCCAC
IKZF3E2_NGS_F	TCGTCGGCAGCGTCAGATG TGTATAAGAGACAGGGAAT TCTGCTGTTAAGTTTTCCG
IKZF3E2_NGS_R	GTCTCGTGGGCTCGGAGAT GTGTATAAGAGACAGCCAG AGAGGAAAGACCTGATGT
IKZF3E4_NGS_F	TCGTCGGCAGCGTCAGATG TGTATAAGAGACAGTTGTG GGTCTCTGCTGTTTGA
IKZF3E4_NGS_R	GTCTCGTGGGCTCGGAGAT GTGTATAAGAGACAGAGA CATTGAAGCTGATGCAGGA

Genomic DNA extractions and next-generation amplicon sequencing

Genomic DNA was extracted from at least 50,000 cells/sample five days after transfections using QuickExtract DNA extraction solution (Lucigen) according to the manual. Amplicons of interest were analyzed from genomic DNA samples on a NextSeq platform (Illumina). In brief, genomic sites of interest were amplified in a first round of PCR using primers that contained NGS forward and reverse adapters (Table 3). The first PCR was set up using NEBNext Q5 Hot Start HiFi PCR Master Mix (New England Biolabs) in 15 µL reactions, with 0.5 µM of primers and 1.5 µL of genomic DNA. PCR was carried out applying the following cycling conditions: 98 °C for 2 min, 5 cycles of [98 °C for 10 s, annealing temperature for each pair of primers for 20 s (calculated for genomic binding regions of primers by NEB Tm Calculator), and 65 °C for 10 s], then 25 cycles of [98 °C for 10 s, 98 °C for 20 s, and 65 °C for 10 s], followed by a final 65 °C extension for 5 min. PCR products were purified using HighPre PCR Clean-up System (MagBio Genomics) and correct PCR product size and DNA concentration was analyzed on a Fragment Analyzer (Agilent). Unique Illumina indexes were added to PCR products in a second round of PCR using KAPA HiFi Hotstart Ready Mix (Roche). Indexing primers were added in a second PCR step and 1 ng of purified PCR product from the first PCR was used as template in a 50 µL reaction volume. PCR was performed applying the following cycling conditions: 72 °C for 3 min, 98 °C for 30 sec, then 10 cycles of [98 °C for 10 s, 63 °C for 30 s, and 72 °C for 3 min], followed by a final 72 °C extension for 5 min. Final PCR products were purified using HighPre PCR Clean-up System (MagBio Genomics) and analyzed by Fragment analyzer (Agilent). Libraries were

quantified using Qubit 4 Fluorometer (Life Technologies), pooled and sequenced on a NextSeq instrument (Illumina). Sequencing data were analyzed by CRISPResso2(Clement et al., 2019).

Amplicon-seq analysis

NGS sequencing data were demultiplexed using bcl2fastq software, and individual FASTQ files were analysed using a Perl implementation of the Matlab script described in a previous publication (Li et al., 2021). For the quantification of indel frequencies, sequencing reads were scanned for matches to two 10 bp sequences that flank both sides of an intervening window in which indels might occur. If no matches were located (allowing maximum 1 bp mismatch on each side), the read was excluded from the analysis. If the length of the intervening window was longer or shorter than the reference sequence, the sequencing read was classified as an insertion or deletion, respectively. The frequency of insertion or deletion was calculated as the percentage of reads classified as insertion or deletion within total analysed reads. If the length of this intervening window exactly matched the reference sequence the read was classified as not containing an indel.

Lentiviral transduction in human memory TH17 cells

The lentivirus particles encoding IKZF4-HA for ectopic gene expression was purchased from VectorBuilder. The lentivirus was generated from a third-generation lentivirus system, using the vector pLV-Puro-SFFV-TagBFP2 for IKZF4/HA expression (HA at the C-terminal) Table 4. The customized lentivirus particles were tittered to obtain optimal transduction efficiency (MOI 2) in human memory TH17 cells (purchased lentivirus titer 10 TU/ml). Bulk TH17 cells were activated for 24 hours in in 96 well plates as described in the "T cells culture" section. 100 µL of media was removed, and 100 µl media containing the lentivirus particles with 8 µg/ml of protamine was added to cells. Cells were spinoculated at 1000 *g* for 1 hours at 32 °C. At day 2 after transduction (day 3 after activation), media was changed in presence of IL-2 at 10 U/ml. At day 5 after transduction (day 6 after activation), cells were harvested for analyses.

qPCR based gene-expression analysis

mRNA was extracted from at least 0.1×10^5 cells using the RNeasy Micro kit (Qiagen# 74004) according to the manufacturer's instructions. cDNA was synthesized using High Capacity cDNA Reverse Transcription kit (Applied Biosystems # 4368814) according to the manufacturer's instructions. Real-Time PCR was performed using TaqMan Fast Advanced Master Mix and probes (Table 5) (ThermoFisher) on a QuantStudio 7 Real-Time PCR system (ThermoFisher). Reactions were performed in multiple technical replicates, and results were calculated using the Δ cycle threshold method normalized to expression of the control gene GAPDH or RPLPO otherwise specified.

Table 4 Lentivirus list

Vector name	Encoding protein	VectorBuilder ID
pLV-Puro-SFFV-TagBFP2	none	VB200417-1151aqz
pLV-Puro-SFFV-Tag-BFP2-T2A-hIKZF4/HA	IKZF4/HA	VB200326-6961rfx

Table 5 Real-Time PCR probe list

Taqman probe	Gene	Dye
IKZF1	Hs00958473_m1	FAM-MGB
IKZF3	Hs05037772_s1	FAM-MGB
IKZF4	Hs00223842_m1	FAM-MGB
IL10	Hs00961622_m1	FAM-MGB
IL22	Hs01574154_m1	FAM-MGB
IL17A	Hs00174383_m1	FAM-MGB
IFNG	Hs00989291_m1	FAM-MGB
TNF	Hs01113624_g1	FAM-MGB
IL2	Hs00174114_m1	FAM-MGB
RPLP0	Hs00420895_gH	FAM-MGB
GAPDH	Hs02786624_g1	FAM-MGB
MAF	Hs04185012_s1	FAM-MGB

Statistical analysis

Data, excluding those describing transcriptomics data, were analyzed using GraphPad Prism (version 9.3.1). The statistical significance of differences between two data groups was determined by paired t-test or one-way ANOVA for multiple groups comparison, at a confidence level of 95%. Exact *n* values and error bars used are provided in the figure legends.

NGS methods

Materials and Methods for RNA-seq, ATAC-seq, pathway analysis and scRNA-seq are in Supplemental Material.

Abbreviations

Th	mouse T helper
TH	human T helper
GM-CSF	granulocyte-macrophage colony-stimulation factor
IFNγ	interferon gamma
IBD	inflammatory bowel disease
IL	interleukin
PBMC	peripheral blood mononuclear cell

ROR-γt	retinoid-related orphan receptor γt
IkZF	Ikaros zing-finger family
seq	sequencing
STAT	signal transducer and activator of transcription
SNP	single nucleotide polymorphism
TF	transcription factor
TGFβ	transforming growth factor beta
TNFα	tumor necrosis factor alpha
Treg	regulatory T cell
GSEA	Gene Set Enrichment Analysis
Lena	lenalidomide

Supplementary Information The online version contains supplementary material available at https://doi.org/10.1007/s00018-026-06089-1.

Acknowledgements We thank Dominik Aschenbrenner for sharing his protocol to set up human memory TH17 clone culture; Henric Olsson and Zach Brohawn for managerial support, P30CA023168. ANRJCJC award to S.M.

Authors contribution S.C.and S.M. developed the original idea. S.C. drafted the manuscript and performed most of the experimental work with the help from K.A., R.B., A.C., A.M., S.L, Y.C. and S.V. L.M. drafted the manuscript and performed the analyses for the RNA-seq. L.M. and M.SA. analyzed the scRNA-seq in follicular lymphoma. E.I., P.V and E.F.C. performed bioinformatic analyses for the RNA-seq and ATAC-seq, L.W. contributed to the generation of the figures for the ATAC-seq data. M.F. performed bioinformatic analyses for the Amplicon-seq. M.L. and S.G. performed GSEA analysis. B.Y., ZZ, and M.K., performed bioinformatic analysis for the scRNA-seq data set from Asthma subjects. I.P. and D.J. prepared the scRNA-seq library of T cells isolated from frozen F.L. PBMCs before and after lenalidomide treatment. L.A. analyzed the F.L. scRNA-seq data. K.T. and S.M. supervised the F.L. scRNA-seq study. S.G. and D.J. coordinated sample collection. S.L. designed the gRNAs for CRISPR-Cas9 KO. S.C., U.G, A.L and S.M. prepared the manuscript with input from S.G., M.H., A.R., A.L., F.M., M.M., K.T., C.P. A.R., H.G., M.K., A.L., M.H., and U.G. provided scientific supervision and helped with the study design. AL and S.M. supervised the study.

Funding This work was supported by the AZ Postdoctoral Fellowship to S.C., K.A. and R.B and ARC PGA and ANRJCJC "SwitchKine" award to S.M., and National Institute of General Medical Sciences of the NIH (R35GM138283 to M.K.) and the SIRG Graduate Research Assistantships Award to B.Y. from the Purdue Institute for Cancer Research.

Data availability Data generated from TH17 clones (RNA- and ATAC-seq) may be obtained in accordance with AstraZeneca's data sharing policy described at https://astrazenecagrouptrials.pharmacm.com/ST/Submission/Disclosure. RNA sequencing data from follicular lymphoma patients before and after lenalidomide treatment (GSE158438) are publicly accessible in the GEO database. Single-cell transcriptomic analysis of allergen-specific T cells in allergy and asthma are from GSE146170. scRNAseq data are available on EGA database with the following accession numbers: EGAD50000001529.

Declarations

Ethics approval and consent to participate Healthy donors were recruited from AstraZeneca volunteers and all samples were taken following appropriate blood collection guidelines. All blood donor volunteers signed Informed Consent Form and donation was approved by AstraZeneca's Human Biological Sample Governance Framwork and local Ethic committee Dnr:2019–03307 (033–10). This research utilized PBMC samples from follicular lymphoma (FL) patients who were enrolled in the GALEN clinical trial (NCT01582776). The research protocol was conducted under French legal guidelines and was approved by the local ethics committee.

Consent for publication All participants provided informed consent for the use of their biological samples in research and publication of results in anonymized form.

Conflict of interest S.C., K.A., R.B., S.L., Y.C. and S.V. were fellows of the AstraZeneca R&D postdoc program. S.C., K.A., R.B., A.M., E.I., P.V., S.L., E.F.C., Y.C., S.V., M.F., L.W., H.G., M.M., M.H. and U.G. are or were employees of AstraZeneca and may own stock or stock options. U.G. is currently employed by Novartis.

References

1. Sallusto F, Zielinski CE, Lanzavecchia A (2012) Human Th17 subsets. Eur J Immunol 42:2215–2220
2. Lee Y, Kuchroo V (2015) Defining the functional states of Th17 cells. F1000Res 4:132
3. Oukka M (2008) Th17 cells in immunity and autoimmunity. Ann Rheum Dis 67(Suppl 3):iii26-29
4. Zambrano-Zaragoza JF, Romo-Martinez EJ, Duran-Avelar MJ, Garcia-Magallanes N, Vibanco-Perez N (2014) Th17 cells in autoimmune and infectious diseases. Int J Inflam 2014:651503
5. Kryczek I et al (2009) Phenotype, distribution, generation, and functional and clinical relevance of Th17 cells in the human tumor environments. Blood 114:1141–1149
6. Zhang JP et al (2009) Increased intratumoral IL-17-producing cells correlate with poor survival in hepatocellular carcinoma patients. J Hepatol 50:980–989
7. Su X et al (2010) Tumor microenvironments direct the recruitment and expansion of human Th17 cells. J Immunol 184:1630–1641
8. Zou W, Restifo NP (2010) T(H)17 cells in tumour immunity and immunotherapy. Nat Rev Immunol 10:248–256
9. Laurence A et al (2007) Interleukin-2 signaling via STAT5 constrains T helper 17 cell generation. Immunity 26:371–381
10. Acosta-Rodriguez EV et al (2007) Surface phenotype and antigenic specificity of human interleukin 17-producing T helper memory cells. Nat Immunol 8:639–646
11. Zielinski CE et al (2012) Pathogen-induced human TH17 cells produce IFN-gamma or IL-10 and are regulated by IL-1beta. Nature 484:514–518

12. Gandhi R et al (2010) Activation of the aryl hydrocarbon receptor induces human type 1 regulatory T cell-like and Foxp3(+) regulatory T cells. Nat Immunol 11:846–853
13. Hu D et al (2017) Transcriptional signature of human pro-inflammatory T(H)17 cells identifies reduced IL10 gene expression in multiple sclerosis. Nat Commun 8:1600
14. Aschenbrenner D et al (2018) An immunoregulatory and tissue-residency program modulated by c-MAF in human T(H)17 cells. Nat Immunol 19:1126–1136
15. Gokhale AS, Gangaplara A, Lopez-Occasio M, Thornton AM, Shevach EM (2020) Corrigendum to "Selective deletion of Eos (Ikzf4) in T-regulatory cells leads to loss of suppressive function and development of systemic autoimmunity" [J. Autoimmun. 105C (<pubYear>2019</pubYear>) 102300]. J Autoimmun 114:102544
16. Evans HG et al (2014) TNF-alpha blockade induces IL-10 expression in human CD4+ T cells. Nat Commun 5:3199
17. Lee Y et al (2012) Induction and molecular signature of pathogenic TH17 cells. Nat Immunol 13:991–999
18. Acosta-Rodriguez EV, Napolitani G, Lanzavecchia A, Sallusto F (2007) Interleukins 1beta and 6 but not transforming growth factor-beta are essential for the differentiation of interleukin 17-producing human T helper cells. Nat Immunol 8:942–949
19. Annunziato F et al (2007) Phenotypic and functional features of human Th17 cells. J Exp Med 204:1849–1861
20. Maggi L et al (2012) Distinctive features of classic and nonclassic (Th17 derived) human Th1 cells. Eur J Immunol 42:3180–3188
21. Wang Y et al (2014) The transcription factors T-bet and Runx are required for the ontogeny of pathogenic interferon-gamma-producing T helper 17 cells. Immunity 40:355–366
22. Noster R et al (2014) IL-17 and GM-CSF expression are antagonistically regulated by human T helper cells. Sci Transl Med 6:241ra280
23. Arshad T, Mansur F, Palek R, Manzoor S, Liska V (2020) A double edged sword role of interleukin-22 in wound healing and tissue regeneration. Front Immunol 11:2148
24. Kim J et al (1999) Ikaros DNA-binding proteins direct formation of chromatin remodeling complexes in lymphocytes. Immunity 10:345–355
25. Powell MD, Read KA, Sreekumar BK, Oestreich KJ (2019) Ikaros zinc finger transcription factors: regulators of cytokine signaling pathways and CD4(+) T helper cell differentiation. Front Immunol 10:1299
26. Quintana FJ et al (2012) Aiolos promotes TH17 differentiation by directly silencing Il2 expression. Nat Immunol 13:770–777
27. Bernardi C et al (2021) CD4(+) T cells require Ikaros to inhibit their differentiation toward a pathogenic cell fate. Proc Natl Acad Sci USA 118
28. Umetsu SE, Winandy S (2009) Ikaros is a regulator of Il10 expression in CD4+ T cells. J Immunol 183:5518–5525
29. Soroosh P et al (2014) Oxysterols are agonist ligands of RORgammat and drive Th17 cell differentiation. Proc Natl Acad Sci USA 111:12163–12168
30. Cheng Y et al (2010) KRAB zinc finger protein ZNF382 is a proapoptotic tumor suppressor that represses multiple oncogenes and is commonly silenced in multiple carcinomas. Cancer Res 70:6516–6526
31. Chen EY et al (2013) Enrichr: interactive and collaborative HTML5 gene list enrichment analysis tool. BMC Bioinformatics 14:128
32. Stubbington MJ et al (2015) An atlas of mouse CD4(+) T cell transcriptomes. Biol Direct 10:14
33. Kronke J et al (2014) Lenalidomide causes selective degradation of IKZF1 and IKZF3 in multiple myeloma cells. Science 343:301–305
34. Lu G et al (2014) The myeloma drug lenalidomide promotes the cereblon-dependent destruction of Ikaros proteins. Science 343:305–309
35. Menard C et al (2021) Lenalidomide triggers T-cell effector functions in vivo in patients with follicular lymphoma. Blood Adv 5:2063–2074
36. Bauche D et al (2020) IL-23 and IL-2 activation of STAT5 is required for optimal IL-22 production in ILC3s during colitis. Sci Immunol 5
37. Lin JX et al (2012) Critical role of STAT5 transcription factor tetramerization for cytokine responses and normal immune function. Immunity 36:586–599
38. Bending D et al (2009) Highly purified Th17 cells from BDC2.5NOD mice convert into Th1-like cells in NOD/SCID recipient mice. J Clin Invest 119:565–572
39. Rieder SA et al (2015) Eos is redundant for regulatory T cell function but plays an important role in IL-2 and Th17 production by CD4+ conventional T cells. J Immunol 195:553–563
40. Mioso G, Gnesotto L, Russo I, Piaserico S, Alaibac M (2023) Exacerbation of psoriasis induced by lenalidomide in a patient with multiple myeloma. J Dermatolog Treat 34:2182619
41. De Novellis D et al (2024) Lenalidomide-induced psoriasis in a refractory multiple myeloma patient successfully treated with narrowband ultraviolet B. Photodermatol Photoimmunol Photomed 40:e12965
42. Chandar R et al (2022) Post-transplant strategies to improve relapse-free survival in childhood leukemia: whole blood donor lymphocyte infusions and lenalidomide for inducing graft-versus-leukemia effect. Pediatr Transplant 26:e14293
43. Kawamura K (2023) Maintenance therapy after allogeneic hematopoietic stem cell transplantation for patients with multiple myeloma. Int J Hematol 118:193–200
44. Besnard AG et al (2012) Inflammasome-IL-1-Th17 response in allergic lung inflammation. J Mol Cell Biol 4:3–10

Authors and Affiliations

Silvia Cerboni[1] · Leila Mohammadnezhad[2] · Komal Agrawal[1] · Ramachandramouli Budida[1] · Ilenia Papa[3] · Silvia Gaggero[2] · Joel Dulong[3] · Anna Cole[4] · Anja Mezger[5] · Bingyu Yan[6] · Zonghao Zhang[7] · Elisabeth Israelsson[1] · Petr Volkov[8] · Songyuan Li[5] · Eva F. Caceres[8] · Malo Leprohon[2] · Mojtaba Shekarkar Azgomi[2] · Yue Cui[1] · Svitlana Salemio[1] · Mike Firth[9] · Leif Wigge[8] · Anna Rudin[10] · Hanna Grindebacke[11] · Marcello Maresca[5] · Chrystal Paulos[4] · Franck Morschhauser[12] · Salomon Manier[2,12] · Majid Kazemian[6,12] · Arian Laurence[13] · Michael Hühn[14] · Ulf Gehrmann[1] · Karin Tarte[3] · Suman Mitra[2]

✉ Michael Hühn
Michael.Huhn@astrazeneca.com

✉ Suman Mitra
suman.mitra@inserm.fr

1 Translational Science and Experimental Medicine, Research and Early Development, Respiratory and Immunology (R&I), BioPharmaceuticals R&D, AstraZeneca, Gothenburg, Sweden

2 PERSTIM Lab, CRCLille, Inserm U1366, CNRS UMR9020 ONCOLille, University of Lille, Institut Pasteur Lille (IPL), Lille, France

3 UMR1236, Department of Immunology, Rennes I University, Rennes, France

4 Winship Cancer Institute, Emory University School of Medicine, Atlanta, GA 30322, USA

5 Translational Genomics, Discovery Sciences, BioPharmaceuticals R&D, AstraZeneca, Gothenburg, Sweden

6 Department of Biochemistry, Purdue University, West Lafayette, IN, USA

7 Department of Agricultural and Biological Engineering, Purdue University, West Lafayette, IN, USA

8 Data Sciences and Quantitative Biology, Discovery Sciences, BioPharmaceuticals R&D, AstraZeneca, Gothenburg, Sweden

9 Data Sciences and Quantitative Biology, Discovery Sciences, BioPharmaceuticals R&D, AstraZeneca, Cambridge, UK

10 Department of Rheumatology and Inflammation research, The Sahlgrenska Academy at Gothenburg University, Gothenburg, Sweden

11 Late-stage development, Respiratory and Immunology (R&I), BioPharmaceuticals R&D, AstraZeneca, Gothenburg, Sweden

12 Department of Hematology, CHU de Lille, Lille, France

13 Translational Gastroenterology Unit, Experimental Medicine Division, John Radcliffe Hospital, Oxford, UK

14 Bioscience, Research and Development, Respiratory and Immunology (R&I), BioPharmaceuticals R&D, AstraZeneca, Gothenburg, Sweden